[16]N. C. Dutta, C. Matsubara, R. T. Pu, and T. P. Das, Phys. Rev. 177, 33 (1969).
[17]E. S. Chang, R. T. Pu, and T. P. Das, Phys. Rev. 174, 1 (1968); 174, 16 (1968).
[18]J. D. Lyons, R. T. Pu, and T. P. Das, Phys. Rev. 178, 103 (1969).
[19]T. S. Lee, N. C. Dutta, and T. P. Das, Phys. Rev. (to be published).
[20]All values for polarizabilities are quoted in a.u. In obtaining refractive indices from them we have used $N_0 = 0.26870 \times 10^{20}$ and the Bohr radius $a_0 = 5.29167 \times 10^{-9}$ cm. from Phys. Today 71, 48 (1964).
[21]D. A. Johnston, C. J. Oudemans, and R. H. Cole, J. Chem. Phys. 33, 1310 (1960).
[22]E. Clementi, IBM J. Res. Develop. 9, 2 (1965).
[23]Z. Kopal, Numerical Analysis (John Wiley & Sons, Inc., New York, 1961).
[24]H. A. Bethe and E. E. Salpeter, Quantum Mechanics of One- and Two-Electron Systems (Academic Press Inc., New York, 1957), p. 18.
[25]C. Cuthbertson and M. Cuthbertson, Proc. Roy. Soc. (London) A135, 40 (1932).
[26]A. Dalgarno and A. E. Kingston, Proc. Roy. Soc. (London) A259, 424 (1960).
[27]The experimental values of the transition frequencies are tabulated by Charlotte E. Moore, National Bureau of Standards Circular No. 467 (U. S. Government Printing Office, Washington, D.C., 1949), Vol. 1.

PHYSICAL REVIEW A VOLUME 1, NUMBER 3 MARCH 1970

Hyperfine Structure of the 2^3S_1 State of He^3†*

S. D. Rosner† and F. M. Pipkin
Lyman Laboratory, Harvard University, Cambridge, Massachusetts 02138
(Received 18 July 1969)

The zero-field hyperfine structure of the metastable 2^3S_1 state of He^3 has been measured by the optical pumping magnetic resonance method. The hyperfine transitions in a weak magnetic field were observed at low temperature in order to achieve narrow linewidths. Discussions of the theory of the hyperfine structure, the theory of the experiment, the apparatus, and the experimental procedure are presented. The final value for the hyperfine structure is 6 739 701 177 ± 16 Hz on the A-1 time scale. The fractional pressure shift of the hyperfine structure is $(-7.4 \pm 3.0) \times 10^{-9}$/Torr. The theoretical and experimental values for the hyperfine structure are compared, and the dependence on the nuclear structure is discussed.

INTRODUCTION

One of the important sources of information concerning nuclear and atomic structure is precision measurements of hyperfine structure intervals. The theoretical value for the hyperfine structure (hfs) depends upon knowledge of the atomic and nuclear wave functions, the electrodynamic corrections, and the values for the fundamental constants. One of the fundamental hyperfine intervals is that for He^3 in the metastable 2^3S_1 state. The hyperfine interval for this simple atomic state should be calculable to high precision; the agreement between the calculations and the measured interval can be used to test quantum electrodynamics and atomic-structure calculations.

This paper reports a redetermination of the hyperfine structure of the metastable 2^3S_1 state of He^3. The previous measurements of this hyperfine structure interval used an atomic-beam technique.[1,2] The precision of the measurements was limited by the transit time through the radio-frequency field; the linewidth was 40–55 kHz. The experiment reported here used an optical pumping technique to measure the hyperfine structure. The precision of the measurements was limited by exchange collisions between atoms in the metastable state and atoms in the ground state; the linewidth was 1–2 kHz. This large decrease in linewidth made it possible to reduce by more than an order of magnitude the error in the hyperfine structure interval.

The optical orientation of metastable He^3 was first reported by Colegrove, Schearer, and Walters.[3] They also showed that the cross section for exchange of metastability with the 1^1S_0 ground-state atoms was high enough to transfer the orientation to the ground state. This rapid metastability exchange process has the undesirable effect of severely broadening the magnetic resonance lines of the metastable state when the gas is at room temperature. It was predicted by Buckingham and Dalgarno[4,5] and demonstrated experimentally by Colegrove, Schearer, and Walters[6] that the metastability exchange cross section decreases rapidly as the temperature is decreased. The consequent narrowing of the metastable resonance lines has made possible a measurement of the hyperfine structure interval to a

precision of 3 parts in 10^9.

This paper deals in sequence with the theory of the He^3 hyperfine structure, the He^3 optical pumping, the apparatus, the experimental procedure, the results, and the relation of the results to the existing theory. In addition to a value for the hyperfine structure, measurements of the light shift and pressure shift of the hyperfine structure interval are reported.

THEORY OF HYPERFINE STRUCTURE

The corrections to the zero-order expression for the hyperfine structure of the 2^3S_1 state in He^3 have been calculated by various authors. The purpose of this section is to summarize these corrections.

The Hamiltonian for the Fermi contact interaction is[7]

$$H_F = \tfrac{16}{3}\pi \mu_B \mu_{nuc} [\vec{S}_1 \cdot \vec{I}\delta^3(\vec{r}_1) + \vec{S}_2 \cdot \vec{I}\,\delta^3(\vec{r}_2)]. \quad (1)$$

Here, μ_B is the Bohr magneton, μ_{nuc} is the He^3 nuclear magnetic moment, $\vec{I}$ is the nuclear spin operator, $\vec{S}_i$ is the spin operator for the ith electron, and $\vec{r}_i$ is the position vector of the ith electron relative to the nucleus. The expression in brackets can be rewritten in the form

$$\tfrac{1}{2}\vec{S}\cdot\vec{I}\,[\delta^3(\vec{r}_1) + \delta^3(\vec{r}_2)] + \tfrac{1}{2}(\vec{S}_1 - \vec{S}_2)\cdot\vec{I}[\delta^3(\vec{r}_1) - \delta^3(\vec{r}_2)], \quad (2)$$

where $\vec{S} = \vec{S}_1 + \vec{S}_2$.

The second operator in Eq. (2) has vanishing diagonal matrix elements but contributes a small correction in second order.

Since the nuclear spin of He^3 is $\frac{1}{2}$, the coupling of the electronic and nuclear angular momenta gives rise to total angular momenta F of $\frac{3}{2}$ and $\frac{1}{2}$. The hyperfine structure is the separation at zero field of the $F=\frac{3}{2}$ and $F=\frac{1}{2}$ states. In the 2^3S_1 state of He^3, one electron is in an $n=1$, $l=0$ hydrogenic state, and the other electron is in an $n=2$, $l=0$ hydrogenic state. Since the hyperfine structure for a hydrogenic electron with quantum numbers nl goes as $n^{-3}(2l+1)^{-1}$, the lowest-order approximation simply neglects the second electron. That is, it neglects $\delta^3(\vec{r}_2)$ in Eq. (2). The expectation value of the remaining term in Eq. (2) gives, for the hyperfine structure,[7]

$$\Delta\nu^0(He^3, {}^3S_1) = 32\alpha^2 c R_\infty (\mu_{nuc}/\mu_e)\tfrac{1}{2} g_e \text{ Hz}. \quad (3)$$

Here α is the fine-structure constant, c is the velocity of light, μ_e is the magnetic moment of the free electron, R_∞ is the Rydberg for infinite mass, and g_e is the gyromagnetic ratio of the free electron. We now consider the corrections to $\Delta\nu^0$.

A. Nonrelativistic Effects of the Second Electron

From Eq. (2) it can be seen that the largest correction for the second electron is a factor

$$1+\epsilon = \frac{\int |\psi(\vec{r}_1,\vec{r}_2)|^2[\delta^3(\vec{r}_1)+\delta^3(\vec{r}_2)]\,d^3r_1 d^3r_2}{\int |\psi_{1s}(\vec{r}_1)|^2\delta^3(\vec{r}_1)\,d^3r_1}, \quad (4)$$

$$1+\epsilon = \tfrac{1}{4}\pi\int |\psi(\vec{r}_1,0)|^2 d^3r_1 . \quad (5)$$

Here $\psi(\vec{r}_1,\vec{r}_2)$ is the exact nonrelativistic wave function for the 2^3S_1 state. Through the use of a variational method, Pekeris obtained for $1+\epsilon$ the value[8]

$$1+\epsilon = 1.0370045 . \quad (6)$$

The estimated uncertainty is 5 parts in 10^8.

The second term of Eq. (2) connects singlet and triplet states; it shifts the hyperfine levels of the 2^3S_1 state by mixing in a part of the 2^1S_0 state. Sternheim has calculated this effect to be[9]

$$\Delta_2 = -9.89 \pm 0.04 \text{ ppm} . \quad (7)$$

B. Relativistic Corrections to the Wave Function

Sessler and Foley[10] calculated the correction to the hyperfine structure of the form $1+\delta\alpha^2$ which arises from the use of wave functions which satisfy an approximate form of the Dirac equation. They considered each electron to be in an effective field and made an additional modification to take into account the exclusion principle. They obtained for δ:

$$\delta_{1s} = 6.06 \text{ ppm} , \quad (8)$$

$$\delta_{2s} = 2.83 \text{ ppm} . \quad (9)$$

The relativistic correction to the hyperfine splitting is

$$\Delta_{rel} = \left(\frac{\delta_{1s}|\psi_{1s}(0)|^2 + \delta_{2s}|\psi_{2s}(0)|^2}{2\int|\psi(\vec{r},0)|^2 d^3r_1}\right)\alpha^2 . \quad (10)$$

The use of Hartree wave functions for ψ_{1s} and ψ_{2s} gives

$$\Delta_{rel} = 5.91\alpha^2 = 315 \pm 3 \text{ ppm}. \quad (11)$$

C. Radiative Corrections

The radiative or quantum-electrodynamic corrections to the hyperfine structure have been summarized by Brodsky and Erickson.[11-13] There are two parts to these corrections – one is the correction to the free-electron g factor, and the other is the quantum-electrodynamic corrections to the hyperfine structure of S states. Since most of the hyperfine structure arises from the $1s$ electron at distances from the nucleus comparable to the Compton wavelength, screening is negligible, and one can use the results for a hydrogenic atom in a $1s$ state with the nuclear charge Z set equal to 2. The theoretical value for the free-electron g factor is[14]

$$g_e = 2[1 + \alpha/2\pi - 0.3285\alpha^2/\pi^2 + 0.13\alpha^3/\pi^3 + \cdots] \ . \tag{12}$$

Combining this with the other quantum-electrodynamic corrections to the hyperfine structure of S-state atoms gives for the total correction[13]

$$\begin{aligned}\Delta_{ed} &= (\alpha/2\pi) - 0.328\,(\alpha/\pi)^2 - (\tfrac{5}{2} - \ln 2)\alpha(Z\alpha) \\ &\quad - (2/3\pi)\alpha(Z\alpha)^2 \ln^2(Z\alpha)^{-2} \\ &\quad + (\tfrac{37}{72} + \tfrac{4}{15} - \tfrac{8}{3}\ln 2)(1/\pi)\,\alpha(Z\alpha)^2 \ln(Z\alpha)^{-2} \\ &\quad + (18.36 \pm 5)(1/\pi)\,\alpha(Z\alpha)^2 \ .\end{aligned} \tag{13}$$

Evaluation yields

$$\Delta_{ed} = (948.2 \pm 2.5) \text{ ppm} \ . \tag{14}$$

The coefficients of the last two terms of Eq. (13) depend upon the atomic state. The uncertainty is estimated on the basis of the expected size of the uncalculated terms; it is expressed in terms of the coefficient of the $\alpha(Z\alpha)^2$ term.

D. Corrections Due to Nuclear Structure and Motion of the Nucleus

The replacement of the electron mass by the reduced mass changes the distance scale of the wave function by a factor of $(1 + m/M)$. This in turn multiplies the expectation value of the Fermi contact interaction [Eq. (1)] by $(1 + m/M)^{-3}$. This is the largest correction due to nuclear motion.[7]

A relativistic treatment of the electron-nucleus interaction gives terms of the form

$$\alpha(m/M)\ln(M/m) \ .$$

These terms have been calculated for He^{3+} by Greenberg and Foley using a noncovariant perturbation scheme.[15] If the second electron is neglected, one can use the He^{3+} result for the problem of interest here. This gives

$$\Delta\alpha m/M = -29 \pm 3 \text{ ppm} \ . \tag{15}$$

Important corrections to the hyperfine structure arise from the spatial distribution of the nuclear currents and the nuclear magnetic moments. Sessler and Foley[10] have calculated these corrections for He^3 and He^{3+}. They argue that, to high precision, the nuclear structure corrections to the hyperfine structure should be the same. The motions of the two electrons in the neighborhood of the nucleus should be substantially independent, thus making the evaluation of the wave function in this region a one-electron problem. Also, any correction for the second electron should be down by the probability that it will also be in the nuclear region.

The largest correction comes from the adiabatic approximation to the electron motion. Sessler and Foley begin with adiabatic approximation and assume that, in the region of the nucleus, the electron moves much faster than the nucleons and takes up an orbit centered about the instantaneous position of the two protons. The electron wave function obtained in this manner is then matched at large distances to the solution which describes motion about the center of mass of the nucleus. Since the correct nuclear wave functions are unknown, Sessler and Foley use two different forms of the nuclear wave function – one due to Hughes and the other due to Pease and Feshbach. They use either a crude variational principle or a fit to the "Coulomb energy" difference between He^3 and H^3 to determine the free parameter in the Hughes solution. They obtain corrections to the hyperfine structure ranging from -146 to -183 ppm. This correction will be symbolized by Δ_{ss}. Thus,

$$-183 \text{ ppm} \leq \Delta_{ss} \leq -146 \text{ ppm} \ . \tag{16}$$

The -183 ppm was calculated using the wave function which reproduced the $He^3 - H^3$ Coulomb energy difference.

There is an admixture of about 3% D state in the nuclear wave function. Sessler and Foley use the Russell-Saunders approximation to calculate this contribution; they neglect the dipole-dipole part of the hyperfine interaction. Using the radial dependence of the Pease-Feshbach function, they obtain for the D-state contribution

$$\Delta_{Dn} = 2.9 \text{ ppm} \ , \tag{17}$$

$$\Delta_{Dp} = -4.2 \text{ ppm} \ , \tag{18}$$

and for the net D-state contribution

$$\Delta_D = \Delta_{Dn} + \Delta_{Dp} - 0.03\,\Delta_{ss} = 3.3 \text{ ppm} \ . \tag{19}$$

A modification to the adiabatic approximation to take into account the motion of the c.m. of the two protons and their relative motion yields a correction

$$\Delta_{\text{nad}} = 11.7 \text{ ppm} \ . \tag{20}$$

The contribution to the hyperfine structure due to the nuclear orbital motion is

$$\Delta_{\text{nc}} = 0.78 \text{ ppm} \ . \tag{21}$$

Sessler and Foley also try to estimate a correction to the hyperfine structure due to meson interaction currents. This calculation is not reliable and they give estimates in the range

$$-230 \text{ ppm} \leq \Delta_{\text{ic}} \leq -2.0 \text{ ppm} \ . \tag{22}$$

We shall not include this correction in our evaluation of the He^3 hyperfine splitting.

Sessler and Mills[16] have calculated the effect of the electromagnetic structure of the proton and neutron on the hyperfine structure. Using the values 0.80 ∓ 0.04 F and 0.70 ± 0.10 F for the electromagnetic rms radii of the proton and neutron, respectively, they obtain the relative correction

$$\Delta_{\text{nes}} = -13 \pm 2 \text{ ppm} \ . \tag{23}$$

This result is based on a parametrization of the nuclear wave function which is obtained by equating the difference in binding energy between He^3 and H^3 to the Coulomb energy. Another choice of parameters gives -16 ± 2 ppm.

In terms of these component corrections, the total nuclear correction is

$$\Delta_{\text{nuc}} = \Delta_{\text{ss}} + \Delta_D + \Delta_{\text{nad}} + \Delta_{\text{nc}} + \Delta_{\text{nes}} + \Delta_{\text{ic}} \ . \tag{24}$$

We shall assume Δ_{ic} is zero.

Sessler and Foley[10] have also calculated the effect of diamagnetic shielding. They obtained a correction

$$\Delta_{\text{dm}} = 4.3 \text{ ppm} \ . \tag{25}$$

In terms of these corrections, the final expression for the He^3 hyperfine splitting is

$$\Delta\nu(\text{He}^3, 2^3S_1) = 32\alpha^2 cR_\infty (\mu_{\text{nuc}}/\mu_e)\tfrac{1}{2}g_e \times (1 + m/M)^{-3}(1 + \epsilon)(1 + \Delta_2 + \Delta_{\text{rel}} + \Delta_{\text{ed}} + \Delta\alpha m/M + \Delta_{\text{nuc}} + \Delta_{\text{dm}}) \ . \tag{26}$$

All of these corrections are summarized in Table I. Taking for the fundamental constants the values [17-19]

$$\alpha^{-1} = 137.03602(21) \ (1.5 \text{ ppm}) , \tag{27}$$

$$c = (2.997925(10) \times 10^{10} \text{ cm/sec} \ (0.33 \text{ ppm}), \tag{28}$$

$$R_\infty = (109\,737.312(11) \text{ cm}^{-1} \ (0.1 \text{ ppm}) , \tag{29}$$

$$(\mu_{\text{He}^3}/\mu B) = (\gamma_{\text{He}^3}/\gamma_p)(\mu_p/\mu_B) \ , \tag{30}$$

$$(\gamma_{\text{He}^3}/\gamma_{\text{p}}) = 0.7618120(7) \ (1 \text{ ppm}) \ , \tag{31}$$

$$(\mu_{\text{p}}/\mu_B) = 1.52103264(46) \times 10^{-3} \ (0.30 \text{ ppm}) , \tag{32}$$

$$m = (5.485930(34) \times 10^{-4} \text{amu} \ (6.2 \text{ ppm}) , \tag{33}$$

$$M = 3.01603 \text{ amu}, \tag{34}$$

$$\tfrac{1}{2}g_e = 1 + (\alpha/2\pi) - 0.3285(\alpha/\pi)^2 + 0.13(\alpha/\pi)^3 , \tag{35}$$

$$\tfrac{1}{2}g_e = 1.0011596389(19) \ (0.0019 \text{ ppm}) , \tag{36}$$

$$1 + \epsilon = 1.03700450(5) \ (0.05 \text{ ppm}) \ , \tag{37}$$

we can write

$$\Delta\nu(\text{He}^3, 2^3S_1) = (6.7326415 \times 10^9 \pm 2.4 \text{ ppm})(1 + \Delta)Hz \times (1 + \Delta)\text{Hz} \ . \tag{38}$$

If we take $\Delta_{\text{ss}} = -183$ ppm ,

$$\Delta = (1\,050.3 \pm 5.3) \text{ ppm} \ ; \tag{39}$$

If we take $\Delta_{\text{ss}} = -146$ ppm ,

$$\Delta = (1087.3 \pm 5.3) \text{ ppm} \ . \tag{40}$$

In the first case,

$$\Delta\nu(\text{He}^3, 2^3S_1) = (6\,739\,712 \pm 39) \text{ kHz} (5.8 \text{ ppm}) \ ; \tag{41}$$

in the second case,

$$\Delta\nu(\text{He}^3, 2^3S_1) = (6\,739\,962 \pm 38) \text{ kHz} (5.8 \text{ ppm}). \tag{42}$$

Another hyperfine structure interval of interest is that of $n = 2$ state of the He^{3+} ion. The Fermi formula gives

$$\Delta\nu^0(\text{He}^{3+}, 2^2S_{1/2}) \tfrac{16}{3} \alpha^2 cR_\infty (\mu_{\text{nuc}}/\mu_e)\tfrac{1}{2}g_e \text{ Hz}. \tag{43}$$

TABLE I. A summary of the corrections to the hyperfine structure of He^3 in the 2^3S_1 state.

Origin	Symbol	Magnitude (ppm)
Presence of second electron	$1+\epsilon$	1.0370045 ± 0.05
Reduced mass	$(1+m/M)^{-3}$	0.999454399 ± 0.003
Second-order contribution	Δ_2	-8.89 ± 0.04
Use of relativistic wave functions	Δ_{rel}	315 ± 3
Quantum-electrodynamic corrections	Δ_{ed}	948.2 ± 2.5
Relativistic reduced mass	$\Delta\alpha m/M$	-29 ± 3
Spin hfs in adiabatic approximation	Δ_{ss}	$-146 \rightarrow -183$
Nuclear D state	Δ_D	3.3
Correction to adiabatic approximation	Δ_{nad}	11.7
Nuclear orbital motion	Δ_{nc}	0.8
Proton and neutron structure	Δ_{nes}	-13 ± 2
Diamagnetic shielding	Δ_{dm}	4.3

With the following exceptions, the corrections to this expression are similar to those for $\Delta\nu \times(He^3, 2^3S_1)$. The corrections $1+\epsilon$, Δ_2, and Δ_{dm} depend specifically on the second electron and do not apply to this problem; the relativistic and radiative corrections change their values in state-dependent terms since the single electron in the ion has $n=2$, whereas the dominant electron in the atom has $n=1$. The corrections are summarized in Table II. The sum is (1196.6 ± 4.4) ppm using $\Delta_{ss} = -183$ ppm, and (1233.6 ± 4.4) ppm using $\Delta_{ss} = -146$ ppm.

The quantity ρ defined as

$$\rho = \Delta\nu(He^3, 2^3S_1)/\Delta\nu(He^{3+}, 2^2S_{1/2}) \qquad (44)$$

depends only on the differences in the corrections and is believed to be independent of the nuclear structure corrections. The theoretical value is

$$\rho = 6.2211157 \pm 0.0000187 \ . \qquad (45)$$

The uncertainty is due primarily to the uncertainty in Δ_{rel}.

TABLE II. A summary of the corrections to the hyperfine structure of He^{3+} in the $2^2S_{1/2}$ state.

Origin	Symbol	Magnitude (ppm)
Use of relativistic wave functions	Δ_{rel}	452.6
Quantum-electrodynamic	Δ_{ed}	952.3 ± 2.5
Relativistic reduced mass	$\Delta(\alpha m/M)$	-29 ± 3
Spin hfs in adiabatic approximation	Δ_{ss}	$-146 \rightarrow -183$
Nuclear D state	Δ_D	3.3
Correction to adiabatic approximation	Δ_{nad}	11.7
Nuclear orbital motion	Δ_{nc}	0.8
Proton and neutron structure	Δ_{nes}	-13 ± 2

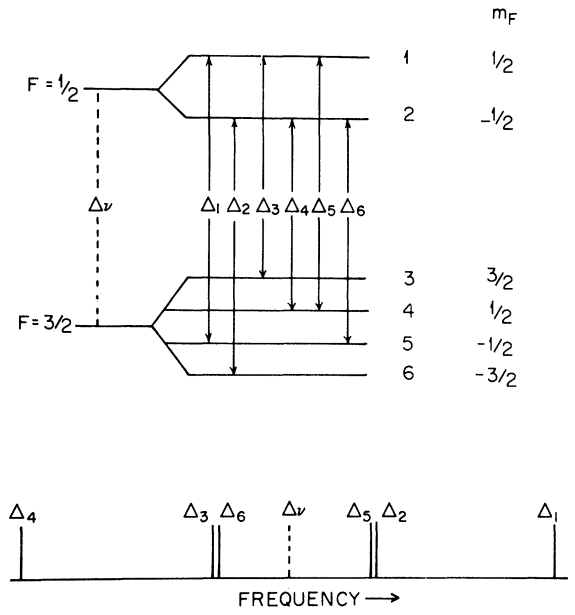

FIG. 1. Energy levels and the hyperfine transitions for a He^3 atom in the 2^3S_1 metastable state.

ENERGY LEVELS OF $^3S_1$ STATE OF He^3

The effective Hamiltonian describing the 2^3S_1 state of He^3 in a magnetic field is

$$H = A\vec{I}\cdot\vec{J} - g_J\mu_B(\vec{J}\cdot\vec{H}) - g_I\mu_B\vec{I}\cdot\vec{H} \ . \qquad (46)$$

Here A is the hyperfine interaction constant, $\vec{J}$ is the electronic angular momentum, $\vec{I}$ is the nuclear angular momentum, g_J is the electronic gyromagnetic ratio, g_I is the nuclear gyromagnetic ratio, and $\vec{H}$ is the external magnetic field. Simple diagonalization of this Hamiltonian gives for the energy levels the expressions:

$$E(\tfrac{1}{2}, \tfrac{1}{2}) = E_1 = \tfrac{1}{6}h\Delta\nu - \tfrac{1}{2}g_J\mu_B H + \tfrac{1}{2}h\Delta\nu \times (1 - \tfrac{2}{3}x + x^2)^{1/2} \ ; \qquad (47)$$

$$E(\tfrac{1}{2}, -\tfrac{1}{2}) = E_2 = \tfrac{1}{6}h\Delta\nu + \tfrac{1}{2}g_J\mu_B H + \tfrac{1}{2}h\Delta\nu \times (1 + \tfrac{2}{3}x + x^2)^{1/2} \ ; \qquad (48)$$

$$E(\tfrac{3}{2}, \tfrac{3}{2}) = E_3 = -\tfrac{1}{3}h\Delta\nu - g_J\mu_B H - \tfrac{1}{2}g_I\mu_B H \ ; \qquad (49)$$

$$E(\tfrac{3}{2}, \tfrac{1}{2}) = E_4 = \tfrac{1}{6}h\Delta\nu - \tfrac{1}{2}g_J\mu_B H - \tfrac{1}{2}h\Delta\nu \times (1 - \tfrac{2}{3}x + x^2)^{1/2} \ ; \qquad (50)$$

$$E(\tfrac{3}{2}, -\tfrac{1}{2}) = E_5 = \tfrac{1}{6}h\Delta\nu + \tfrac{1}{2}g_J\mu_B H - \tfrac{1}{2}h\Delta\nu \times (1 + \tfrac{2}{3}x + x^2)^{1/2} \ ; \qquad (51)$$

$$E(\tfrac{3}{2}, -\tfrac{3}{2}) = E_6 = \tfrac{1}{3}h\Delta\nu + g_J\mu_B H + \tfrac{1}{2}g_I\mu_B H. \qquad (52)$$

Here $x = (g_J - g_I)\mu_B H/h\Delta\nu$, (53)

and $\Delta\nu = -\tfrac{3}{2}(A/h)$. (54)

For He^3, g_J, g_I, and A are negative. Figure 1 depicts graphically the energy levels and the hyperfine transitions for He^3.

PRINCIPLES OF EXPERIMENT

The optical pumping of He^3 has been discussed in detail by Colegrove *et al.*[3]; only a brief review will be given here. Figure 2 shows the relevant energy levels of He^3 in a weak magnetic field.

A weak glow discharge maintained in He^3 gas at a pressure of 0.1 to several Torr populates the metastable 2^3S_1 level so that the density of metastable atoms is roughly 1 in 10^6. If resonance radiation at 1.08 μ, corresponding to the $2^3P_J \times (J = 0, 1, 2) \rightarrow 2^3S_1$ transitions, illuminates the metastable atoms, the absorption of the resonance light followed by re-emission to the metastable state produces an inequality in the populations of

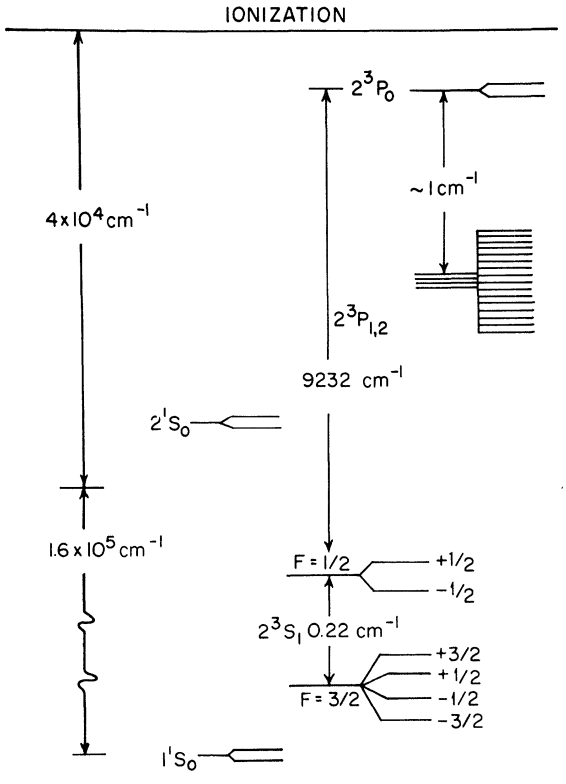

FIG. 2. Energy levels of the He^3 atom relevant to the optical pumping processes.

the magnetic sublevels of the metastable state. As the metastable state becomes oriented, the atoms become less absorbing and the light transmitted by the absorption cell increases. If a radio-frequency field is now applied so as to equalize the populations of the sublevels, the atoms become more absorbing and the light transmitted by the absorption cell decreases. Thus, the light transmitted by the cell can be used to monitor the orientation and to detect the radio-frequency transitions.

The observed signal can be expressed in the form

$$S(\Delta\omega, H_1) = I(\Delta\omega, H_1) - I(0, 0) \ . \tag{55}$$

Here, $I(\Delta\omega, H_1)$ is the light absorbed per second by the metastable atoms when the amplitude of the rotating radio-frequency field is H_1 and the frequency deviation from resonance is $\Delta\omega/2\pi$. $I(0, 0)$ is the light absorbed when no rotating field if present.

An expression for $S(\Delta\omega, H_1)$ which gives the correct dependence on $\Delta\omega$ and H_1 can be obtained for the case where only one pair of levels is affected by the radio-frequency field. This is realized experimentally in the hyperfine transitions with $F=1$, $m_F=0, \pm1$. The model is a two-level metastable state illuminated by resonance radiation, connected by an H_1 field, and coupled to a two-level ground state by metastability exchange collisions. The labeling of the energy levels is depicted graphically in Fig. 3.

The absorption coefficients of the two states for the incident light are b_1 and b_2. It is convenient to express them in terms of a pumping time τ_p such that $B_i = B_i/\tau_p$, where B_i is a relative absorption coefficient. If the normalization $\Sigma_1 B_i = 2$ is chosen, then $1/\tau_p$ becomes the mean number of photons absorbed per atom per unit time, as is conventional. We assume for simplicity the case of complete mixing in the excited-state sublevels, so that an atom excited from either of the two metastable levels has an equal chance of returning to either level. The equation of motion for the density matrix describing this system is

$$\dot{\rho}_{11} = \frac{1}{2\tau_r}(\rho_{22} - \rho_{11}) - \left(\frac{B_1}{2\tau_p} + \frac{1}{\tau_m}\right)\rho_{11} + \frac{B_2}{2\tau_p}\rho_{22} + \frac{1}{T_m}\rho_{aa} + \frac{i}{\hbar}[\rho_{12}H_{21} - H_{12}\rho_{21}], \tag{56}$$

$$\dot{\rho}_{22} = -\frac{1}{2\tau_r}(\rho_{22} - \rho_{11}) - \left(\frac{B_2}{2\tau_p} + \frac{1}{\tau_m}\right)\rho_{22} + \frac{B_1}{2\tau_p}\rho_{11} + \frac{1}{T_m}\rho_{bb} - \frac{i}{\hbar}[\rho_{12}H_{21} - H_{12}\rho_{21}], \tag{57}$$

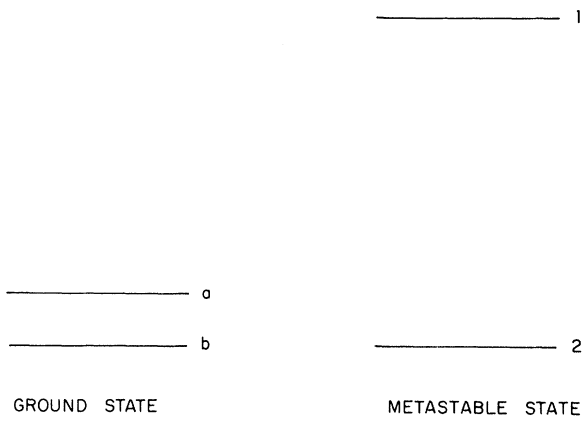

FIG. 3. Energy levels for and the notation for the model system using a two-level metastable atom with a two-level ground state.

$$\dot{\rho}_{12} = -\left(\frac{1}{\tau_2} - i\omega_0\right)\rho_{12} + \frac{i}{\hbar}(\rho_{11} - \rho_{22})H_{12} \ , \tag{58}$$

$$\dot{\rho}_{aa} = \frac{1}{2T_r}(\rho_{bb} - \rho_{aa}) + \frac{1}{\tau_m}\rho_{11} - \frac{1}{T_m}\rho_{aa}, \tag{59}$$

$$\dot{\rho}_{bb} = -\frac{1}{2T_r}(\rho_{bb} - \rho_{aa}) + \frac{1}{\tau_m}\rho_{22} - \frac{1}{T_m}\rho_{bb} \ . \tag{60}$$

Here $$H_{12} = \langle 1 | H(t) | 2 \rangle = \gamma\hbar H_1 \cos\omega t \ , \tag{61}$$

where γ is the transition g factor. The definitions of the various relaxation times are as follows: τ_r is the relaxation time for polarization of metastable atoms, τ_p is the mean time between photon absorptions for a metastable atom, τ_m is the mean time between metastability exchange collisions for a metastable atom, τ_2 is the relaxation for off-diagonal elements of the density matrix describing the metastable atoms, T_m is the mean time between metastability exchange collisions for a ground-state atom, and T_r is the relaxation time for polarization of ground-state atoms. τ_2 is not independent of the other relaxation times. It can be written as

$$\frac{1}{\tau_2} = \frac{1}{\tau_p} + \frac{1}{\tau_r} + \frac{1}{\tau_m} + \frac{1}{\tau_2'} \ , \tag{62}$$

where τ_2' is the additional relaxation due to pure dephasing collisions. The terms in $1/T_m$ and $1/\tau_m$ have been constructed in accordance with collisions of the form

$$He^m(2) + He^g(a) \rightleftarrows He^m(1) + He^g(b) \ , \tag{63}$$

and it has been assumed that no coherence is preserved in the exchange collisions.

Straightforward solution of these equations gives in the steady state

$$S(\Delta\omega, H_1) = \tfrac{1}{2}(b_1 - b_2)(1 - B_2) \times \frac{(\tau_1/\tau_p)\tau_1\tau_2(\gamma H_1)^2}{1 + (\tau_2\Delta\omega)^2 + \tau_1\tau_2(\gamma H_1)^2}$$

$$= \frac{1}{\tau_p}(1 - B_2)^2 \frac{(\tau_1/\tau_p)\tau_1\tau_2(\gamma H_1)^2}{1 + (\tau_2\Delta\omega)^2 + \tau_1\tau_2(\gamma H_1)^2} , \quad (64)$$

where $$\frac{1}{\tau_1} = \frac{1}{\tau_p} + \frac{1}{\tau_r} + \frac{1}{\tau_m}\left(\frac{T_m}{T_m + T_r}\right) . \quad (65)$$

The linewidth, defined as the full width at half-amplitude of the signal, is

$$\Delta\omega_{1/2} = 2\left[\left(\frac{1}{\tau_2}\right)^2 + \frac{\tau_1}{\tau_2}(\gamma H_1)^2\right]^{1/2} . \quad (66)$$

The signal at saturation ($H_1 \to \infty$) is

$$S(\Delta\omega, \infty) = (1 - B_2)\tau_1/\tau_p{}^2 \text{ photons/sec} . \quad (67)$$

The pumping time is given by the expression

$$\frac{1}{\tau_p} = \int_0^\infty I_\nu \sigma_\nu d\nu = I_0 \int_0^\infty \sigma_\nu d\nu . \quad (68)$$

Here I_ν is the spectral density of the incident light in photons/cm^2 sec unit frequency range, I_0 is its value at the center of the absorption line, and σ_ν is the cross section for absorption of a photon of frequency ν by an atom when the magnetic sublevels are equally populated.

No attempt was made to obtain detailed information concerning I_ν. However, some qualitative statements can be made. Following Colegrove *et al.*[3] we have used light from a He^4 lamp to pump He^3. Because of the isotope shift, to a good approximation only the intense D_1 and D_2 components of the He^4 emission are absorbed by the D_0 transition in He^3. Furthermore, Greenhow[20] has shown that the He^4 emission pumps principally the $F = \frac{3}{2}$ level of the metastable state. For the lamp used in this experiment,

$$I_0 \simeq 2\times10^{15} \text{ photons/cm}^2 \text{ sec Hz} ,$$

and $$\tau_p = 3.3\times10^{-3} \text{ sec} .$$

The reduction of the linewidth is a prime concern in a high-precision measurement of the hyperfine structure. The major contributions to the linewidth are light absorption, collision processes, and Doppler broadening. We shall treat each of them in this order.

The removal of the 2^3S_1 atoms from the metastable state by photon absorption to the 2^3P_0 level constitutes a lifetime limiting process which broadens the resonance line. The linewidth is predicted to be

$$\Delta\nu_{1/2}(\text{light}) = 1/\pi\tau_p = 100 \text{ Hz} .$$

The light contribution measured in the experiment was 220 Hz.

The contribution of collision processes to τ_2 may be summarized as

$$\left(\frac{1}{\tau_2}\right)_{\text{coll}} = \frac{1}{\tau_r} + \frac{1}{\tau_m} .$$

The relaxation time τ_r summarizes those processes which destroy the polarization of the metastable atoms, such as spin exchange collisions between metastable atoms and free electrons present in the bulb. In addition, there may be processes which quench the metastable atoms to the ground state and thus limit the lifetime of the atoms. Quenching of metastables out of the glow discharge which produces them has been studied by Phelps and Molnar.[21] They found lifetimes as long as 20 msec at room temperature. Measurements of the linewidth of the Zeeman transitions in He^4 at room temperature give a metastable lifetime of approximately 10^{-4} sec. 20 msec gives a linewidth of 18 Hz; 10^{-4} sec gives a linewidth of 3.3 kHz.

The most important collisional relaxation time is τ_m; it is due to metastability exchange collisions. Calculations[5,22,23] of the interaction between metastable He atoms and ground-state He atoms show that there is a small repulsive barrier of roughly 0.2 eV at a separation of $4a_0$. The existence of this barrier is confirmed by the dramatic decrease in the metastability exchange cross section at low temperatures.[6,24] The linewidth goes from 80 kHz at room temperature to 0.8 kHz at 15 °K.

The Doppler broadening is reduced by the presence of the buffer gas.[25] For a bulb filled to 0.163 Torr at 273 °K the mean free path at 4.2 °K is 1.4×10^{-2} cm. The wavelength of the microwave field that drives the resonance is 4.45 cm. Thus, the expected width due to Doppler broadening is 92 Hz.

APPARATUS

Figure 4 shows a schematic picture of the apparatus. In order to reduce the linewidth due to metastability collisions it was necessary to cool

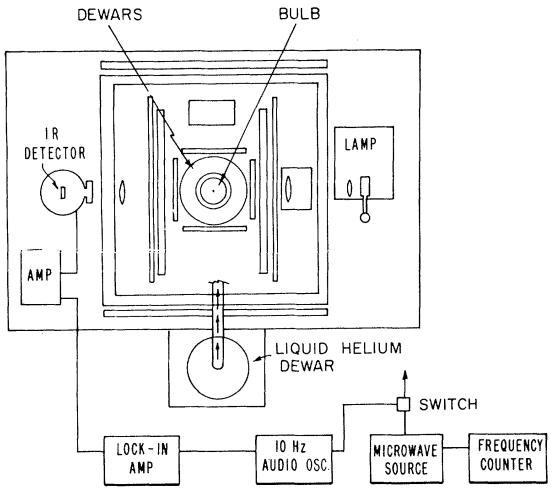

FIG. 4. Schematic diagram of the optical pumping apparatus.

the bulb down to temperatures in the neighborhood of 15 °K. This made it necessary to put the bulb in a Dewar system and provide cryogenic cooling. The main parts of the apparatus are the resonance lamp, the detector, the sample bulb, the discharge system, the cryogenic system, the magnetic field correction system, the frequency source for driving the hyperfine transitions, and the equipment for measuring the frequency. We shall deal with each of these in the order in which they are listed.

The 1.08-μ resonance radiation was produced by a He^4 filled Pyrex disc-shaped bulb excited in the plate coil of a 40-W 100-MHz oscillator. For a disc lamp having a $1\frac{1}{2}$ in. diameter and a 0.375 in. inside thickness, a helium pressure of 1.5 Torr (at 27 °C) was found to be optimum. Since the lamp operates at temperatures greater than 200 °C, the disc was joined to a Pyrex reservoir in order to buffer the pressure against diffusion losses. The lamp oscillator was driven by regulated high-voltage supplies and the filament was run from a regulated supply. This reduced the light-source noise below the level of vibration and detector noise. A particularly obnoxious source of noise was dust particles in the light beam; the heat from the light source produced thermal currents which stirred up the dust and made it dance. Care was taken to keep the light path clean and to keep all of it covered.

The detector was a lead sulfide photoconductor (Ektron, Eastman Kodak Co.). Because of its enhanced signal-to-noise ratio at low temperatures, the detector was cooled to dry-ice temperature by mounting it on a copper cold finger in a stainless-steel Dewar. Good thermal contact with the cold finger was achieved by coating the back of the glass substrate of the detector with Apiezon L vacuum grease. Because of the reported loss of sensitivity in an oxygen-free atmosphere, the detector was not constantly maintained under vacuum.

The detector circuit is shown in Fig. 5. Since the detector resistance increases to more than 20 MΩ at dry-ice temperature, an ultrahigh input impedance IGFET was used to provide a low output impedance to the low-level amplifier which followed (Tektronix 122). Because the detector response time is poor at low temperatures, the modulation frequency was set at 10 Hz.

Figure 6 shows a typical sample bulb. The bulbs were fabricated of Pyrex and provided with two glass covered tungsten electrodes for producing the discharge. The electrode seals have survived over 10 cyclings to 15 °K without failing. Precautions were taken to clean the bulb thoroughly in order to reduce the pump-down time and ensure no degradation of signal due to impurity collisions. The bulbs were rinsed with hot nitric

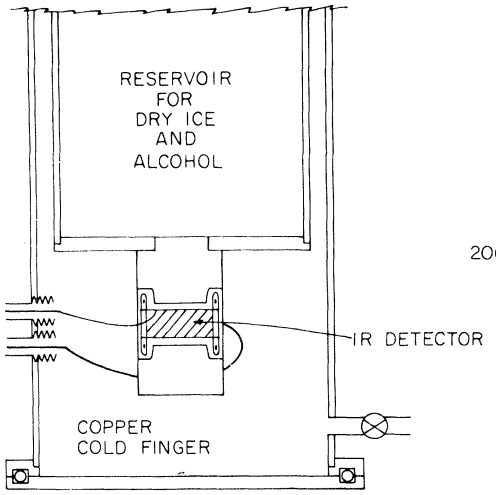

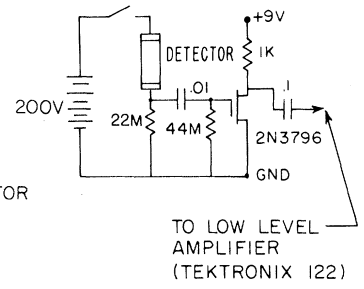

FIG. 5. Diagram showing the circuit used to match the high-impedance detector to the Tektronix 122 preamplifier.

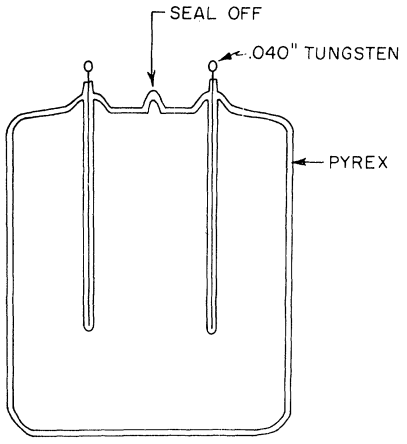

FIG. 6. Typical absorption bulb.

acid or a room-temperature solution of hydrofluoric acid and nitric acid to remove visible traces of grease and dirt. After a thorough rinse with tap and distilled water, they were sealed into a Pyrex and stainless vacuum system and evacuated with baking to a pressure of 10^{-3} Torr. Final cleaning was done by valving off the pump and admitting He^4 gas to a pressure of a few Torr. A bright glow discharge was ignited and after a few minutes the gas was pumped out. After one or two such flushing cycles, the bulb was filled to the desired pressure with He^3 gas which had been purified by flowing it through a liquid helium cold trap and a barium-coated quartz tube. In some cases, the gas was further purified by running a discharge in a titanium-coated bulb adjacent to the sample bulb. A sample of He^3 gas so treated was examined spectroscopically and found to have an impurity level of less than 10 ppm.

A 50-MHz Colpitts oscillator coupled to the bulb electrodes produced a weak glow discharge in the bulb. It was especially important to maintain the discharge at the weakest point at which it would sustain itself stably because strong discharges not only provided shorter relaxation times for the metastables but also heated the gas and thus broadened the line through metastability exchange collisions. Actual measurements of the gas temperature as a function of discharge strength confirmed this. The rf power was conducted to the bulb by a simple twin wire transmission line constructed of fine stainless wire with teflon spacers. Ignition of the discharge occurred either spontaneously or with the momentary application of a Tesla coil to the transmission line at the oscillator.

The bulb was mounted, as shown in Fig. 7, and inserted into a cryostat constructed from two glass Dewars. The inner Dewar was a standard Pyrex Dewar silvered everywhere except for a cylindrical band to pass the pumping light. This Dewar was located inside a similarly silvered outer Dewar. The outer Dewar was filled with liquid nitrogen to a point just below the bottom of the unsilvered band. Thus, no bubbling liquid nitrogen was ever in the path of the pumping light. The discharge bulb was cooled by using a heater to boil off He gas from a liquid-helium storage Dewar and passing the gas through a vacuum-jacketed transfer tube to the bottom of the inner Dewar. With a liquid-helium consumption of roughly 1 to 2 liters h, this system was capable of cooling the bulb to a temperature of 15 °K when there was a discharge in the bulb. The bulb temperature was first monitored only by measuring the linewidth of the $F=\frac{3}{2}$ Zeeman transitions using the results of Colegrove *et al.*[6] to estimate the temperature. In later work, the temperature was monitored to a precision of about 1 °K using a carbon resistor as a thermometer. The details of this together with the data on the linewidth versus temperature will be presented elsewhere.

The great advantage of the gaseous cooling system was the absence of bubbles which could severely modulate the light transmission and produce random noise much larger than the signal amplitude. At very high flow rates of the cooling gas, a component of noise behaving in this way was observed; at the actual flow rates used, this gas

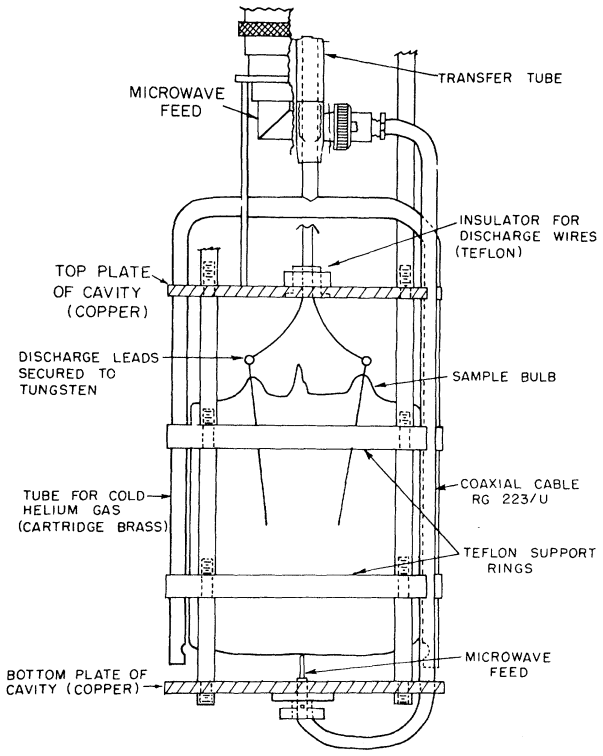

FIG. 7. Mounting system for the absorption bulbs.

noise was negligible compared with modulation of the light intensity by vibration and dust particles.

The mount for the bulb also had provisions for a transmission line to supply the microwave radiation to the bulb. A thin-walled stainless-steel coaxial line with teflon spacers was connected to a flexible coaxial cable terminating in a circular loop under the bulb. A low-Q cavity was provided by the copper plates forming the top and bottom of the bulb holder. The top plate together with a set of copper baffles insulated the bulb against a convection heat leak from room temperature.

The experiment was carried out in the earth's magnetic field with no magnetic shielding. The vertical component of the earth's field was cancelled by a set of rectangular Helmholtz coils. Local inhomogeneities in the horizontal component which would broaden the resonance lines excessively were corrected by three electrical shim coils based on a design of Anderson.[26] These shims were easily and independently adjustable to compensate for any local changes in the magnetic field at the bulb. The shimming was done using a standard Rb optical pumping system as a magnetometer. The He^3 bulb was replaced by a Rb bulb of similar shape and size mounted in an identical manner. The shims were set to minimize the linewidth of the Zeeman transitions in Rb^{85} and $Rb.^{87}$ It was possible to reduce the field-dependent linewidth for Rb^{87} to 60 Hz; this corresponds to a field variation of 0.08 mG over the illuminated volume of roughly 150 cm^3.

Stray 60-cycle fields were large in the vicinity of the experiment due to the proximity of some ac current mains. The amplitudes of the fields were 1 and 5 mG, respectively, for the components parallel and perpendicular to the horizontal component of the earth's field. The 1-mG field was sufficient to produce severe frequency modulation of the resonance lines, which appeared as a series of peaks and valleys superimposed on the Lorentzian line shape. This structure confused the task of measuring the position of the resonance line center precisely, and it was necessary to eliminate it. This was done with a negative feedback system similar to that described by Pipkin and Lambert.[27]

It was also necessary to suppress the 60-Hz component perpendicular to the light beam. This component was so large that a slight misalignment of the pickup coils used to sense the horizontal field caused the perpendicular component to be picked up. The resulting correction signal would then overcompensate the horizontal component. Suppression of all the components of 60-Hz fields removed the fm structure from the resonance lines.

The hyperfine transitions lie in the vicinity of 6739.7 MHz and at low temperatures have linewidths of about 1 kHz. Thus, to measure the line center to $\frac{1}{50}$ of the linewidth requires an oscillator stability of 2 parts in 10^9. This was achieved by the conventional technique of phase-locking a klystron to an accurately known stable frequency standard. In this case, we used a 1-MHz signal produced in the laboratory of J. A. Pierce of the Harvard University J. A. Division of Engineering and Applied Physics. The stability of the signal is constantly checked by comparison with independent atomic-frequency standards and by observing the correction that must be applied to slave the 1-MHz oscillator to a harmonic of the standard 20 kHz signal transmitted by WWVL. The 1-MHz signal is assigned a stability of a few parts in 10^{11} over several weeks.

The 1-MHz standard was multiplied in three stages to a value of 6736 MHz with conventional frequency-locked oscillators (Gertsch AM-1, FM4). The 6736 MHz was mixed with a 20 dB sample of the klystron output, and the intermediate frequency (i.f.) of 3.7 ± 0.5 MHz was amplified and compared with a local oscillator (General Radio 616-D) in a phase detector. The dc output of the phase detector was fed through a low-pass filter and added in series with the dc reflector voltage thus completing the feedback loop. This system was capable of locking the klystron over a range of 500 kHz and for an average of 15 min before a slight manual adjustment of the reflector voltage was required to restore phase-lock. The existence of phase-lock was monitored by observing on an oscilloscope the Lissajous pattern produced by the reference and the i.f. signal.

A Hewlett Packard HPA 3503 diode switch driven by a Schmitt trigger circuit and an audio oscillator was used to chop the microwave power at a frequency of 10 Hz. The signals were demodulated with a lock-in detector. The signals could also be recorded on a Brown recorder.

MEASUREMENT PROCEDURE AND RESULTS

A typical run proceeded as follows. About 2 h before the time suitable for taking data, the klystron and stabilization circuitry was turned on. While the electronics was warming up, the transfer tube and the detector Dewar were pumped out to 10^{-5} Torr using a liquid-nitrogen-trapped oil diffusion pump. The transfer tube was connected to the bulb mount and the bulb was inserted in the inner Dewar. Room-temperature helium gas was flowed through the transfer tube and inner Dewar to purge the system of air and moisture. The outer Dewar was filled with liquid nitrogen to the bottom of the silvered band. The heater stick was precooled in liquid nitrogen and inserted into the helium storage Dewar. The transfer tube, with the attached bulb mount, was raised out of the experimental Dewar and inserted simultaneously into the liquid-helium storage Dewar and the exper-

imental Dewar. The heater was then turned on and the cooldown started. The time for bringing the bulb to thermal equilibrium was about 0.75 h. The timing was arranged so that data taking could begin about 1:30 a.m. It has been found that there is a significant reduction to magnetic noise arising from automobiles, trolleys, and other experiments between 1:30 a.m. and 6:00 a.m.

The discharge was turned on and the linewidths of the Zeeman and hyperfine transitions measured. When the linewidth of the hyperfine transitions stabilized at about 2 kHz, the frequency measurements were begun. A pair of transitions with equal but opposite linear field dependence was selected and their frequencies measured. One observer used the lock-in amplifier to adjust the klystron frequency so as to maximize the signal; the other observer recorded the frequency. Each line was measured four times in succession; then the other line of the pair was measured four times. The average of these eight numbers produced one measurement of the hyperfine splitting. After making two such determinations of the hyperfine frequency, the two observers changed places. This process was continued until the increase in environmental noise made it difficult to make precise measurements. All the measurements reported here were made using unpolarized light.

The pairs of transitions Δ_1, Δ_4, or Δ_2, Δ_3 can be used to determine the zero-field hyperfine splitting. From Eqs. (47)–(53), it can be easily shown that, to order $x^2\Delta\nu$,

$$\Delta\nu = \tfrac{1}{2}(\Delta_1 + \Delta_4) - \frac{2}{9}\frac{(\Delta_1 - \Delta_4)^2}{\Delta_1 + \Delta_4} \quad , \tag{69}$$

$$\text{and} \quad \Delta\nu = \tfrac{1}{2}(\Delta_2 + \Delta_3) - \frac{(\Delta_2 - \Delta_3)^2}{\Delta_2 + \Delta_3} \, .$$

The signals for Δ_2, Δ_3 were about 2.5 times greater than those for Δ_1, Δ_4 for the same microwave power. We shall refer to Δ_2, Δ_3 as the strong (S) transitions and to Δ_1, Δ_4 as the weak (W) transitions. Because of the lack of a high-Q cavity to define the mode structure, and hence the magnetic-field direction in the bulb, it was expected that both $\Delta m_F = \pm 1$ and $\Delta m_F = 0$ transitions would be observed. Thus, due to the near degeneracy of Δ_5 with Δ_2 and Δ_6 with Δ_3, these $\Delta m_F = 0$ transitions could distort the line shape of the S transitions and produce a systematic error. This would be especially true if the ratio of the amplitudes of Δ_5 and Δ_2 was different from the ratio of the amplitudes of Δ_6 and Δ_3. In this case, the two asymmetric lines would have different shapes and the average of the line maxima would be in error. For unpolarized light, one expects the signal amplitudes of each member of the pair to be the same; this was one of the reasons for using unpolarized light.

In bulbs with pressure around 0.1 Torr at 0 °C, the signals were large and good measurements could be made of the weak transitions. For bulbs with pressure about 1 Torr at 0 °C, the signals were weaker by a factor of 3 than those at 0.1 Torr. The signal-to-noise ratio for the W transitions was found to be too small to make precise measurements. It was, thus, necessary to use the S transitions in the higher-pressure bulbs and investigate the S transitions for systematic shifts.

The S transitions in the earth's field were traced out with a chart recorder. From the field dependence of the overlapping transitions, one expects the overlap of Δ_2 and Δ_5 to show up as a tail to low frequencies and the overlap of Δ_3 and Δ_6 as a tail to high frequencies. Figure 8 shows typical tracings; they suggest the predicted asymmetry. To confirm this, the static field at the sample was increased from 160 to 420 mG. Figure 9 shows the tracing for the Δ_2, Δ_3 transitions at 420 mG. As expected the asymmetry increases at higher fields. For comparison, Fig. 10 shows tracings of the W transitions in the earth's field (160 mG). The lack of asymmetry of the W transitions is good evidence that the asymmetry of the S transitions is due to overlap. An asymmetry due to field inhomogeneity would be more pronounced in the W transitions due to their greater field dependence. To check empirically for systematic error due to overlap, the hyperfine splitting was measured using both the S transitions and the W transitions in a bulb with 0.163 Torr pressure (at 0 °C).

Four sets of measurements were made, three on a bulb with a pressure of 0.163 Torr and one on a bulb with a pressure of 0.98 Torr. Table II summarizes the results of the measurements. Figure 11 gives histograms showing the dispersion of the data and the variation from night to night.

The data were analyzed in two ways. The first method averaged the eight measurements which give one value for the hyperfine splitting, calculated the expected error in this result due to the dispersion of the component measurements, and then used this error as a weighting factor in estimating the average of all the measurements. If Z_i represents one value for the hyperfine splitting and σ_{Z_i} represents the estimated standard deviation, then the final value is given by

$$\bar{Z} = \sum_{i=1}^{N} \sigma_{Z_i}^{-2} Z_i \Big/ \sum_{i=1}^{N} \sigma_{Z_i}^{-2} \, , \tag{70}$$

and the error is

$$(\sigma_{\bar{Z}})^2 = \frac{1}{N-1} \sum_{i=1}^{N} \sigma_{Z_i}^{-2} (Z_i - \bar{Z})^2 \Big/ \sum_{i=1}^{N} \sigma_{Z_i}^{-2} \, . \tag{71}$$

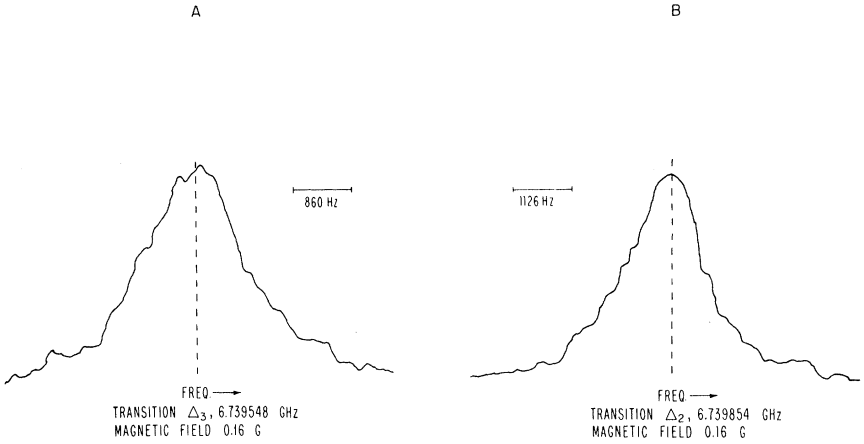

FIG. 8. Recorder tracing of the Δ_2 and Δ_3 hyperfine transitions in a magnetic field of 160 mG (horizontal component of earth's magnetic field). The lock-in-detector time constant was 1.0 sec.

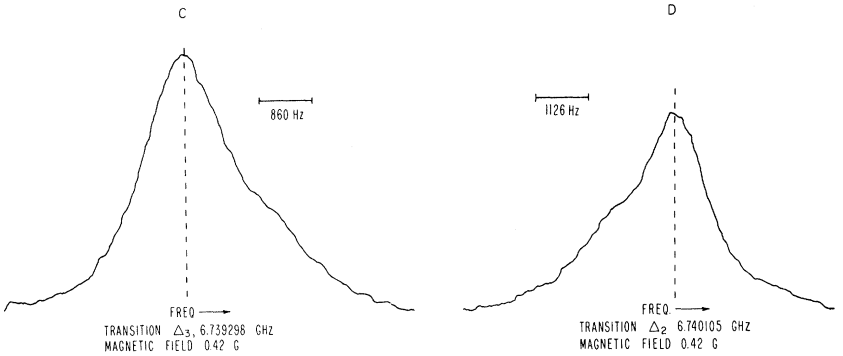

FIG. 9. Recorder tracing of the Δ_2 and Δ_3 hyperfine transitions in a field of 420 mG. The lock-in-detector time constant was 1.0 sec.

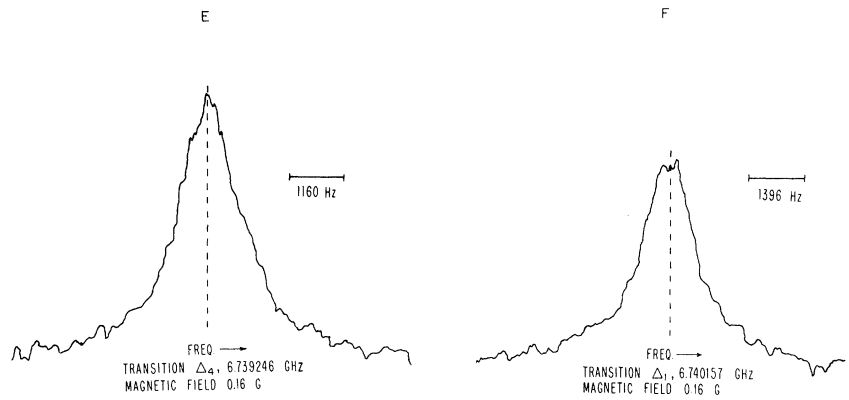

FIG. 10. Recorder tracing of the Δ_1 and Δ_4 hyperfine transitions in a field of 160 mG. The lock-in-detector time constant was 1.0 sec.

The other method weights all the measurements equally and ignores the dispersion of the components of a given measurements. This unweighted mean is

$$Z_\mu = \frac{1}{N} \sum_{i=1}^{N} Z_i \ , \tag{72}$$

and the error

$$(\sigma_{\overline{Z}_\mu})^2 = \frac{1}{N(N-1)} \sum_{i=1}^{N} (Z_i - Z_\mu)^2 \ . \tag{73}$$

The results of both methods of analysis are presented in Table III. The difference of the results gives an estimate of the stability of the result.

The agreement of the measurements on the weak and strong transitions in the 0.163-Torr bulb indicates that any systematic error involved in

TABLE III. A summary of the bulb pressures and the measured values of the hyperfine splitting.

He pressure in Torr at °C	Light intensity (%)	Observed transitions	Number of measurements	Hyperfine splitting ($\Delta\nu - 6\,739\,701\,000$) Hz	
				weighted	unweighted
0.163	100	*W*	42	406.3 ± 9.9	402.9 ± 10.2
	100	*S*	17	401.1 ± 6.0	412.6 ± 5.4
	22	*S*	33	387.6 ± 7.1	388.1 ± 7.9
0.98	100	*S*	35	379.0 ± 12.4	371.9 ± 15.3

using the strong transitions is less than the errors in the measurement. We shall assume that there is no systematic error arising from this source.

Comparison of the measurements on the 0.163-Torr bulb and the 0.98-Torr bulb suggests that there is a small negative pressure shift. A least-squares fit to the measurements made using the unweighted means of the strong transitions gives a zero-pressure intercept of

$$6\,739\,701\,411.0 \pm 10.7 \text{ Hz} \tag{74}$$

and a pressure shift of

$$-50.0 \pm 19.9 \text{ Hz/Torr} . \tag{75}$$

The corresponding fractional pressure shift is

$$(-7.4 \pm 3.0) \times 10^{-9}/\text{Torr} . \tag{76}$$

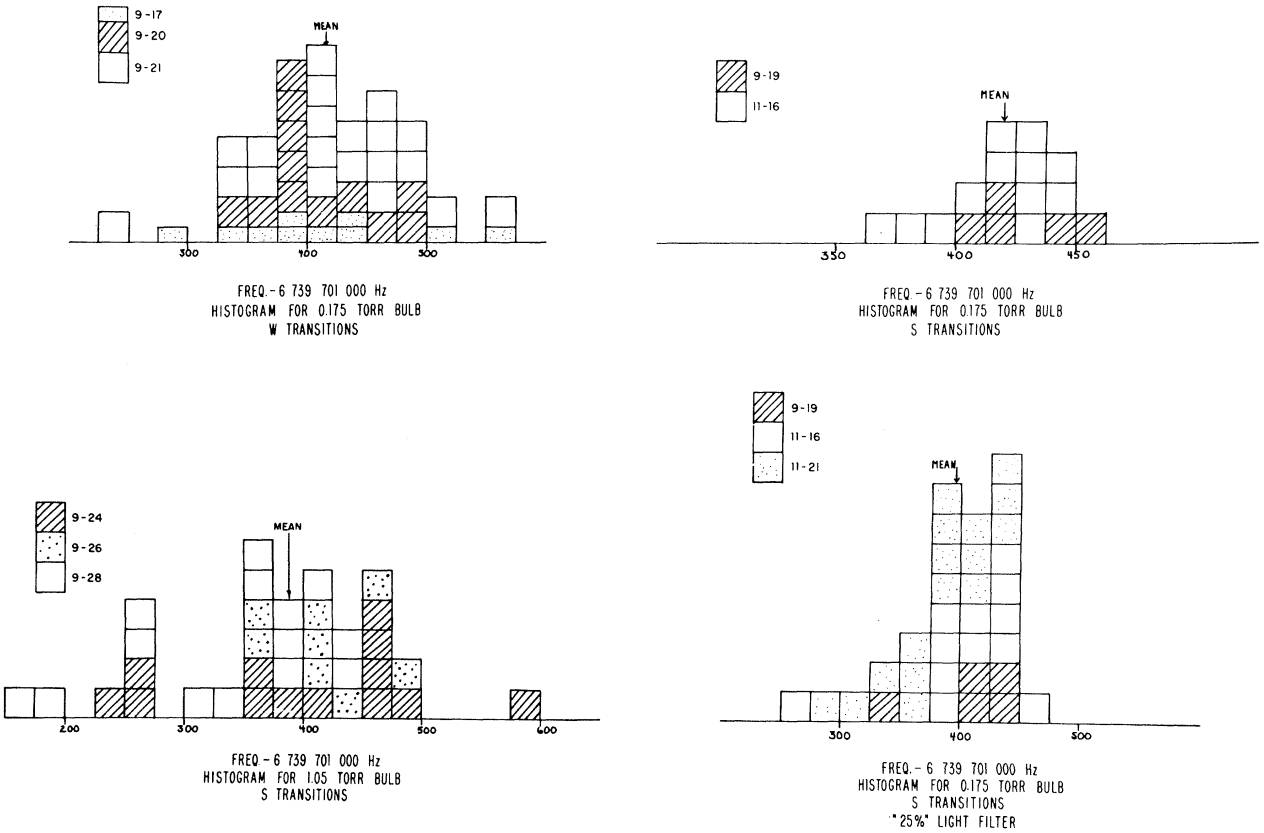

FIG. 11. Histograms showing the distributions of the measurements of the hyperfine splitting. The *W* transitions are Δ_3 and Δ_4; the strong transitions are Δ_1 and Δ_2. These measurements were all made using unpolarized light. The time scale here is *UT*-2 and no quadratic corrections have been made.

The measurements made on the 0.163-Torr bulb with a weaker light intensity suggest that there is a dependence of the hyperfine splitting on the intensity of the pumping light. Using the unweighted mean of this data to extrapolate the zero-pressure hyperfine splitting to zero light intensity, we obtain for the hyperfine splitting of the free He^3 atom in the 2^3S_1 state

$$\Delta\nu(He^3, 2^3S_1) = 6\,739\,701\,379.4 \pm 16.4 \text{ Hz} . \quad (77)$$

The time scale upon which this is based is UT2-1968. To convert this to the A-1 time standard which is based on assigning the hyperfine splitting of Cs^{133} the value

$$\Delta\nu(Cs^{133}) = 9\,192\,631\,770 \text{ Hz}, \quad (78)$$

one multiplies by

$$1 - 3\times10^{-8} . \quad (79)$$

Making this correction, we obtain for He^3 the value

$$\Delta\nu(He^3, 2^3S_1) = 6\,739\,701\,177 \pm 16 \text{ Hz} . \quad (80)$$

CONCLUSIONS

The best previous value of this hyperfine splitting was that measured by White *et al.*,[2] using an atomic beam apparatus. They found

$$\Delta\nu(He^3, 2^3S_1) = 6\,739\,701\,300 \pm 400 \text{ Hz} . \quad (81)$$

This value is in good agreement with that found in this experiment.

The theoretical value for the hyperfine splitting is

$$\Delta\nu(He^3, 2^3S_1)_{\text{theoret}} = (6\,732\,641\,500)(1 + \Delta) \text{ Hz} , \quad (82)$$

where $\Delta = 1050.3 \pm 5.3$ ppm if Δ_{SS} is taken to be -183. The experimental value for Δ is

$$\Delta_{\text{expt}} = 1048.6 \pm 2.4 \text{ ppm} . \quad (83)$$

Here, the error is due primarily to the error in the fine structure constant. The experimental and theoretical values agree very well. This suggests that $\Delta_{SS} = -183$ and that the meson current corrections are small.

One can use the new value of the hyperfine splitting to derive a new value for ρ, the ratio of the hyperfine splitting of the helium ion in the $2^2S_{1/2}$ state to that for the helium atom in the 2^3S_1 state. The best value for the hyperfine structure of the ion is[28]

$$\Delta\nu(He^{3+}, 2^2S_{1/2}) = 1\,083\,354\,990 \pm 200 \text{ Hz} . \quad (84)$$

$$\text{Thus, } \rho_{\text{expt}} = \frac{\Delta\nu(He^3, {}^3S_1)}{\Delta\nu(He^3, {}^2S_{1/2})} = 6.2211384 \pm 0.0000012 . \quad (85)$$

The theoretical value is

$$\rho_{\text{theoret}} = 6.2211157 \pm 0.0000187 . \quad (86)$$

The agreement is satisfactory.

The He^3 measurements are now much more precise than the theory, so there is little motivation to make additional measurements unless the theory is improved.

ACKNOWLEDGMENTS

We are especially indebted to Larry Donaldson for his dedication in building and rebuilding innumerable pieces of glassware so essential to this experiment. We wish to thank J. A. Pierce for making available the standard 1-MHz frequency, the Cryogenics staff of the Cambridge Electron Accelerator for their advice, cooperation, and loan of the heater stick, and the Solid State Group at Gordon McKay Laboratory for the loan of many wave guide components. One of the authors (SDR) wishes to express his gratitude to the National Research Council of Canada for a Fellowship held during part of this work.

---

†Research supported by National Science Foundation Grant Nos. GP 8551 and GP 4353.

*This paper is based on a thesis submitted by one of the authors (SDR) to Harvard University in partial fulfillment of the requirements for the Doctor of Philosophy in Physics.

‡Now at the Clarendon Laboratory, Oxford University, Oxford, England.

[1]G. Weinreich and V. W. Hughes, Phys. Rev. 95, 1451 (1954).

[2]J. A. White, L. Y. Chow, C. Drake, and V. W. Hughes, Phys. Rev. Letters 3, 428 (1959).

[3]F. D. Colegrove, L. D. Schearer, and G. K. Walters, Phys. Rev. 132, 2561 (1963).

[4]R. A. Buckingham and A. Dalgarno, Proc. Roy. Soc. (London) A213, 327 (1952).

[5]R. A. Buckingham and A. Dalgarno, Proc. Roy. Soc. (London) A213, 506 (1952).

[6]F. D. Colegrove, L. D. Schearer, and G. K. Walters, Phys. Rev. 135, A353 (1964).

[7]H. A. Bethe and E. E. Salpeter, Quantum Mechanics of One- and Two-Electron Atoms (Springer-Verlag, Heidleberg, 1957), p. 107.

[8]C. L. Pekeris, Phys. Rev. 126, 1470 (1962).

[9]M. M. Sternheim, Phys. Rev. Letters 15, 545 (1965).
[10]A. M. Sessler and H. M. Foley, Phys. Rev. 98, 6 (1955).
[11]D. E. Zwanziger, Phys. Rev. 121, 1128 (1961).
[12]M. M. Sternheim, Phys. Rev. Letters 15, 336 (1965).
[13]S. J. Brodsky and G. W. Erickson, Phys. Rev. 148, 26 (1966).
[14]R. G. Parsons, Phys. Rev. 168, 1562 (1968).
[15]D. A. Greenberg and H. M. Foley, Phys. Rev. 120, 1684 (1960).
[16]A. M. Sessler and R. L. Mills, Phys. Rev. 110, 1453 (1958).
[17]B. N. Taylor, W. H. Parker, and D. N. Langenberg, Rev. Mod. Phys. 41, 375 (1969).
[18]H. L. Anderson, Phys. Rev. 76, 1460 (1949).
[19]N. F. Ramsey, Phys. Rev. 78, 699 (1950).
[20]R. C. Greenhow, Phys. Rev. 136, A660 (1964).
[21]A. V. Phelps and J. P. Molnar, Phys. Rev. 89, 1202 (1953).
[22]D. J. Klein, E. M. Greenawalt, and F. A. Madson, J. Chem. Phys. 47, 4820 (1967).
[23]H. J. Kolker and H. H. Michels, J. Chem. Phys. 50, 1762 (1969).
[24]W. A. Fitzsimmons, N. F. Lane, and G. K. Walter, Phys. Rev. 174, 193 (1968).
[25]R. H. Dicke, Phys. Rev. 89, 472 (1953).
[26]W. A. Anderson, Rev. Sci. Instr. 32, 241 (1961).
[27]F. M. Pipkin and R. H. Lambert, Phys. Rev. 127, 787 (1962).
[28]R. Novick and E. D. Commins, Phys. Rev. 111, 872 (1958).

PHYSICAL REVIEW A VOLUME 1, NUMBER 3 MARCH 1970

Double Photoionization of Helium

Robert L. Brown
National Radio Astronomy Observatory, * *Green Bank, West Virginia* 24944
(Received 17 October 1969)

The helium double-photoionization cross section has been evaluated using a Hylleraas wave function for the ground state in order to include correlation between the atomic electrons more directly than in previous calculations. Good agreement is found between the present results, the experimental data, and the theoretical work of Byron and Joachain. An interpretation of the differential electron spectrum is used to motivate an asymptotic calculation of the double-photoionization cross section which agrees well with the more exact treatment at high energies.

I. INTRODUCTION

Interest in the helium double-photoionization cross section was stimulated by the observation[1,2] that the oscillator strength for this transition made a non-negligible contribution to the average excitation energy term in the expansion of the Lamb shift. Carlson,[3] who measured the helium double-ionization cross section and noticed that the data could not be interpreted by the electron shake-off process[4] which is based on single electron wave functions, concluded that an adequate description of the data could be obtained only if a many-body approach was employed.

In a series of papers, Byron and Joachain[5,6] arrived at a similar result by pointing out that double ionization depends critically on the way in which correlation effects between atomic electrons are included in the initial-state wave function. These authors expanded the wave function of the bound state of helium in relative partial waves and calculated the double-photoionization cross section[7]; good agreement with Carlson's data was obtained. However, from a comparison with an asymptotic double-ionization calculation,[1] Byron and Joachain estimated the uncertainties in their cross section to be of the order of 25% arising principally from the failure of their ground-state wave function to be of sufficiently high precision.

It is the purpose of this paper to reevaluate the helium double-photoionization cross section using a very accurate Hylleraas wave function for the ground state (Sec. II), and to compare these results with Carlson's data and Byron and Joachain's calculation. An interpretation of the differential cross section is used in Sec. III to stimulate an asymptotic calculation which is found to be applicable at energies greater than 600 eV.

II. DOUBLE-PHOTOIONIZATION CROSS SECTION

Since the double-ionization process depends so critically on correlation of the atomic electrons in the initial state,[4-6] it is important to employ a wave function for the bound state which includes a high degree of correlation: For helium, Hylleraas-type wave functions which explicitly include interelectronic r_{12} terms best fulfill this criterion. In the work that follows, the ground